

Corrosion Behavior of Aluminum in Dilute Acetic Acid Solution Simulating Cooling Water in HVDC Transmission

Peng Zhang^{1,3}, Hao Zhang², Yinsheng Xu², Huixi Li², Jinxiao Liu³, Youping Fan^{1,*}, Shengping Wang^{2,*}

¹ School of Electrical Engineering and Automation, Wuhan University, Wuhan 430072, China

² Faculty of Material Science and Chemistry, China University of Geosciences, Wuhan 430074, China

³ Qujing Bureau, Extra High Voltage Power Transmission Company, China Southern Power Grid Co Ltd, Qujing 655000, China

*E-mail: ypfan@whu.edu.cn, spwang@cug.edu.cn

Received: 9 November 2021 / Accepted: 27 December 2021 / Published: 2 February 2022

The concentration, temperature effect and thermodynamic activation energy of aluminum corrosion in dilute acetic acid solution were explored by the polarization curve and the electrochemical impedance spectroscopy. With the increase of concentration and solution temperature of acetic acid solution, the corrosion resistance and charge transfer impedance of aluminum decreased. From 0 mM to 1.00 mM of acetic acid solution concentration, the corrosion potential, corrosion current density, anodic Tafel slope and charge transfer impedance of aluminum corrosion at 25 °C changed from -1.316 V, 0.207 $\mu\text{A cm}^{-2}$, 5.581 V dec⁻¹, 10.890 k $\Omega \text{ cm}^{-2}$ to -1.141 V, 0.525 $\mu\text{A cm}^{-2}$, 4.264 V dec⁻¹, 7.344 k $\Omega \text{ cm}^{-2}$. And with the solution temperature increase from 25 °C to 55 °C, the corrosion potential, corrosion current, anodic Tafel slope and charge transfer impedance of aluminum in 0.1 mM acetic acid solution changed from -1.248 V, 0.337 $\mu\text{A cm}^{-2}$, 5.387 V dec⁻¹, 9.590 k $\Omega \text{ cm}^{-2}$ to -1.046 V, 1.651 $\mu\text{A cm}^{-2}$, 5.031 V dec⁻¹, 1.633 k $\Omega \text{ cm}^{-2}$. The aluminum corrosion in dilute acetic acid solution was a transition chemical reaction of four processes (diffusion → surface adsorption → surface reaction → desorption).

Keywords: aluminum, corrosion, acetic acid, radiator, high voltage direct current transmission

1. INTRODUCTION

A high voltage direct current (HVDC) transmission system was an efficient way of long-distance energy transmission [1, 2]. The converter valve in HVDC system would generate heat when converting current. The normal working temperature of the converter valve was maintained by aluminum radiator and supporting circulating cooling water system [3, 4]. The inner channel wall of the aluminum radiator exposed to the cooling water with low conductivity was corroded under the action of high electric field, and the formed aluminum ions dissolved in the cooling water and deposited on the surface of platinum

graded electrode [5]. The scale on graded electrode surface increased the contact resistance between the platinum graded electrode and the cooling water, which would seriously affect the normal operation of HVDC transmission system [6, 7].

Inhibiting the corrosion of aluminum radiator in cooling water could effectively slow down and eliminate the scaling of platinum graded electrode [8-11]. There were many reports on the corrosion characteristics of aluminum in electrolyte with low ionic conductivity, such as ammonia [12], carbon dioxide solution [13], sodium bicarbonate solution [14], and ethylene glycol aqueous solution [15]. Like these reports, we still hoped to find a coolant with low ionic conductivity, high specific heat capacity and good electrochemical stability for the valve cooling system of HVDC transmission system.

In recent years, the researches on the corrosion law of metals in organic acid solution were more active. As an organic acid, acetic acid was widely used in daily life, it was of great significance for the development and utilization of aluminum to study the electrochemical corrosion behaviors of aluminum in acetic acid solution. By simulating the working environment of aluminum radiator in HVDC converter valve cooling system, the corrosion behavior of aluminum in low concentration acetic acid solution by electrochemical methods, such as polarization curve and electrochemical impedance spectroscopy (EIS), was studied, and its corrosion mechanism, which provided a theoretical basis for aluminum corrosion protection research in the future was also discussed.

2. EXPERIMENTAL

2.1 Electrochemical system

The three-electrode electrochemical system for testing consisted of a working electrode, a reference electrode, a counter electrode and the acetic acid solution of various concentrations. The platinum black electrode was applied as the counter electrode, and the reference electrode was saturated calomel electrode (SCE). The potential of SCE at 25 °C is 0.228 V (relative to the standard hydrogen electrode (SHE)). The working electrode was aluminum electrode cut from the aluminum radiator, and its exposed working area was 1 cm × 1 cm.

The type number of aluminum was 3003, which consists of Si (0.570 wt%), Fe (0.630 wt%), Cu (0.140 wt%), Mn (1.270 wt%), Zn (0.090 wt%), Li (0.030 wt%) and Al (97.310 wt%). Except for retaining the working surface of 1 cm², all other parts of aluminum immersed in solution were coated with epoxy resin. Before the electrochemical tests, the working electrodes were polished with emery paper and nano-alumina powder, washed several times in distilled water and anhydrous ethanol, and finally placed in a vacuum drying box.

The electrolyte used for aluminum corrosion experiment were 0, 0.05, 0.10, 0.50 and 1.00 mM acetic acid solution, respectively.

2.2 Electrochemical measurements

The steady-state polarization curve and EIS were measured using the CHI 660D electrochemical workstation. The scanning potential rate of aluminum in each electrolyte was 1 mV s^{-1} , and the potential range was 0.800 V (from 0.400 V lower than stable potential to 0.400 V higher than stable potential). The corrosion potential and corrosion current density were obtained from the polarization curves. The corrosion characteristics of aluminum surface were determined by the results of EIS test with the frequency range of 10^{-1} - 10^5 Hz and the amplitude of 5 mV.

The temperatures of thermodynamics test with 0.1 mM acetic acid solution as electrolyte were set at 25, 35, 45 and 55 °C for 5 d, respectively.

Before the electrochemical test of aluminum electrodes, they were immersed in the acetic acid solution with the corresponding test concentration at the corresponding test temperature for 5 d, respectively.

2.3 Physical characterization

The scanning electron microscopy (SEM, Hitachi-S4800) was used to detect the morphologies of the electrode surfaces. The corrosion products were determined by X-ray diffraction (XRD) from 10 ° to 90 ° at a scanning rate of 10 ° min^{-1} with a Rigaku Ultima IV powder diffractometer.

Before the physical characterization of aluminum electrodes, they were immersed in 0.1 mM acetic acid solution for 5 d at 25, 35, 45, 55 °C, respectively.

3. RESULTS AND DISCUSSION

3.1 Concentration effect of aluminum corrosion in acetic acid solution

3.1.1 Potentiodynamic curve analysis

The potentiodynamic curves and corresponding fitting parameters of aluminum in the acetic acid solution are shown in Figure 1 and Table 1. With the increase of acetic acid concentration, the corrosion potential shifted positively and the corrosion current density (I_{corr}) increased. The acetic acid was ionized to form H^+ . With the increase of the acetic acid concentration, the concentration of H^+ increased, and the reaction rate of hydrogen evolution reaction accelerated, leading to the positive shift of corrosion potential. Because the acetic acid concentration changed and the H^+ concentration in the solution increased, the cathodic hydrogen evolution reaction was dominant, and the increase of H^+ concentration accelerated the rate of cathodic reaction [16]. As a result, the resistance of the cathodic reaction was reduced, and the increase of the cathodic reaction rate also promoted the occurrence of the anodic oxygen absorption reaction, so the anodic reaction also increased, and the overall aluminum corrosion rate accelerated.

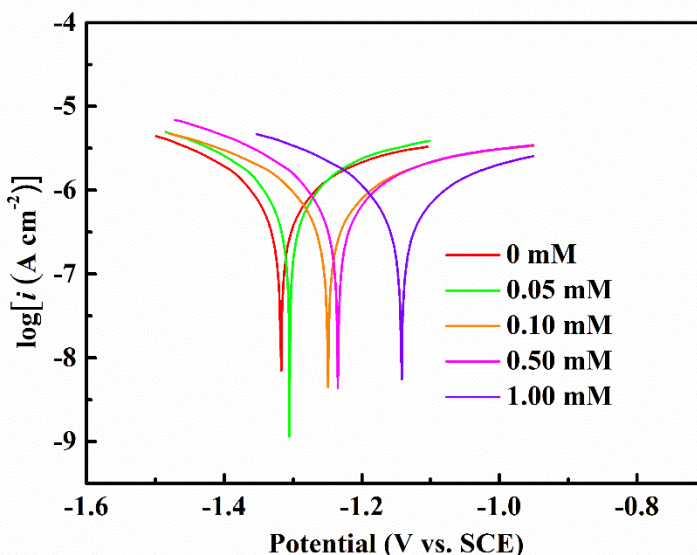


Figure 1. Potentiodynamic curve of aluminum immersed in the acetic acid solution for 5 d at 25 °C

Table 1. Polarization curve parameters of aluminum immersed in the acetic acid solution for 5 d at 25 °C

Concentration (mM)	Corrosion potential E_{corr} (V)	Corrosion current density I_{corr} ($\mu\text{A cm}^{-2}$)
0	-1.316	0.207
0.05	-1.304	0.258
0.10	-1.248	0.337
0.50	-1.235	0.451
1.00	-1.141	0.525

3.1.2 EIS analysis

The EIS curves, the equivalent circuit and their corresponding fitting data of aluminum electrode immersed in the acetic acid solution with various concentrations at 25 °C for 5 d and are shown in Figure 2, Table 2. R_s represents the solution resistance between the reference electrode and the aluminum electrode, C_f , R_f represent the capacitance, charge transfer impedance of the oxide film on the aluminum electrode surface respectively, C_{dl} represents the electric double layer capacitance of the aluminum surface, R_{ct} represents the surface charge transfer resistance of the aluminum, and W represents the diffusion impedance of liquid phase [17].

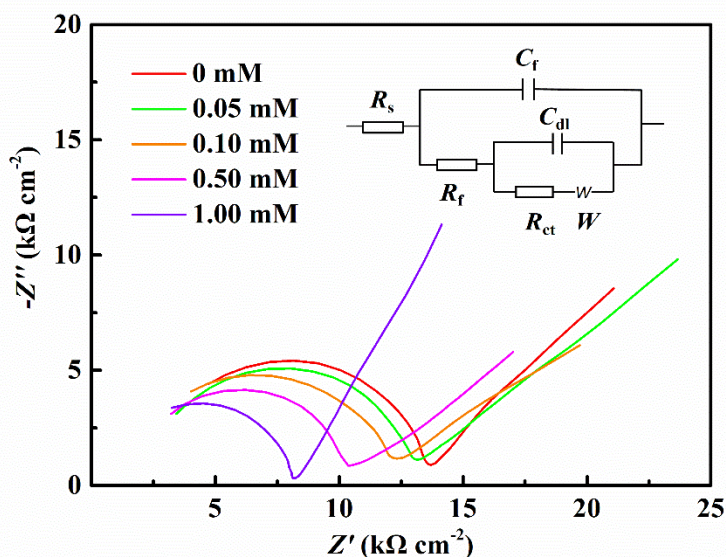


Figure 2. EIS curves of aluminum immersed in the acetic acid solution for 5 d at 25 °C

Table 2. EIS fitting parameters of aluminum immersed in the acetic acid solution for 5 d at 25 °C

Concentration (mM)	R_s ($k\Omega\text{ cm}^{-2}$)	C_f ($nF\text{ cm}^{-2}$)	R_f ($k\Omega\text{ cm}^{-2}$)	C_{dl} ($\mu F\text{ cm}^{-2}$)	R_{ct} ($\Omega\text{ cm}^{-2}$)	W ($\mu\Omega\text{ cm}^{-2}$)
0	2.298	9.860	4.978	1.348	10.890	14.660
0.05	1.776	11.110	5.171	1.410	9.744	15.790
0.10	0.898	12.870	6.565	1.620	9.590	26.970
0.50	0.597	13.353	2.252	1.710	8.229	36.770
1.00	0.345	13.946	2.251	1.926	7.344	10.220

With the increase of acetic acid concentration, the R_s and R_f decreased. This was because the increasing of the acetic acid concentration could increase the number of ions in the solution, thus enhancing the solution conductivity. The increase of solution conductivity led to the decrease of aluminum corrosion resistance. In addition, the C_f and C_{dl} on the aluminum surface increased, and the oxide film capacitance was much smaller than the electric double layer capacitance. This was due to the concentration of acetic acid was low, there were few oxidation products on the aluminum surface, and most of the corrosion products were adsorbed on the aluminum surface in the form of transition ions, resulting in a larger electric double layer capacitance.

3.1.3 Thermodynamic analysis

The tendency and degree of corrosion reaction could be analyzed by thermodynamic parameters, such as Gibbs free energy ΔG^θ , enthalpy change ΔH^θ , entropy change ΔS^θ and equilibrium constant K^θ . The reaction of aluminum in acetic acid solution could be expressed as Equation 1.



In fact, the process of aluminum corrosion reaction in acetic acid solution was carried out in four steps, which was “diffusion” → “surface adsorption” → “surface reaction” → “desorption”. The reaction rate was related to the transition product, so the activation energy of aluminum corrosion reaction in acetic acid solution was obtained from Arrhenius equation [18] (Equations 2, 3).

$$i_{corr} = A \exp\left(\frac{-E_a}{RT}\right) \tag{2}$$

$$\ln i_{corr} = \left(\frac{-E_a}{R}\right) \left(\frac{1}{T}\right) + \ln A \tag{3}$$

Where i_{corr} was the current density of aluminum corrosion reaction in acetic acid solution, E_a was the reaction activation energy, T was the temperature (K), A was the electrochemical constant, R was the gas constant ($8.314 \text{ J mol}^{-1} \text{ K}^{-1}$).

The tendency of corrosion reaction was analyzed from the thermodynamic parameters. In acetic acid solution with various concentrations, the aluminum corrosion reaction were carried out at 25, 35, 45 and 55 °C for 5 d, and then the potentiodynamic curves were tested at each temperature. The activation energy E_a were calculated by with $1000/T$ as the abscissa and the $\ln i_{corr}$ as the longitudinal sites (Table 3).

Table 3. Current density and activation energy of aluminum corrosion reaction in acetic acid solution with various temperatures

Concentration (mM)	Corrosion current density I_{corr} ($\mu\text{A cm}^{-2}$)				E_a (kJ mol^{-1})
	298.15 K	308.15 K	318.15 K	328.15 K	
0	0.207	0.422	0.779	1.368	51.6
0.05	0.258	0.486	0.850	1.500	48.0
0.10	0.337	0.511	0.908	1.651	43.9
0.50	0.451	0.699	1.229	2.207	43.7
1.00	0.525	0.823	1.569	2.438	43.3

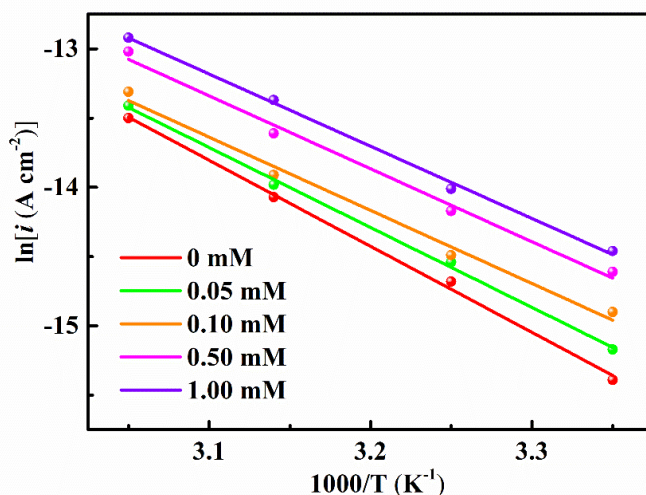


Figure 3. Fitting data of aluminum corrosion reaction in acetic acid solution with various concentrations

With the increase of acetic acid concentration, the activation energy of aluminum corrosion reaction was always positive, suggesting the corrosion and dissolution of aluminum in acetic acid solution needed to absorb energy. In addition, the value of activation energy decreased, indicating that the energy required for corrosion reduced and the tendency of corrosion increased. This conclusion is consistent with the above electrochemical test results.

3.2 Temperature effect of aluminum corrosion in 0.1 mM acetic acid solution

From the above activation energy results, the corrosion and dissolution of aluminum were the processes of absorbing energy, so the ambient temperature had also the effect on the aluminum corrosion. In order to explore the temperature effect of aluminum corrosion, the following experiments were designed.

3.2.1 Potentiodynamic curve analysis

The potentiodynamic curves and fitting data of aluminum in 0.1 mM acetic acid solution at various temperatures are shown in Figure 4 and Table 4. The current density of aluminum corrosion increased with the increase of solution temperature. These results showed that the aluminum corrosion resistance decreased with the increase of temperature. This was because the increase of temperature accelerated the corrosion reaction rate, and the corrosion dissolution of aluminum was an endothermic reaction, the high solution temperature made its equilibrium to the direction of forming corrosion products. Therefore, the high acetic acid solution temperature accelerated the aluminum corrosion.

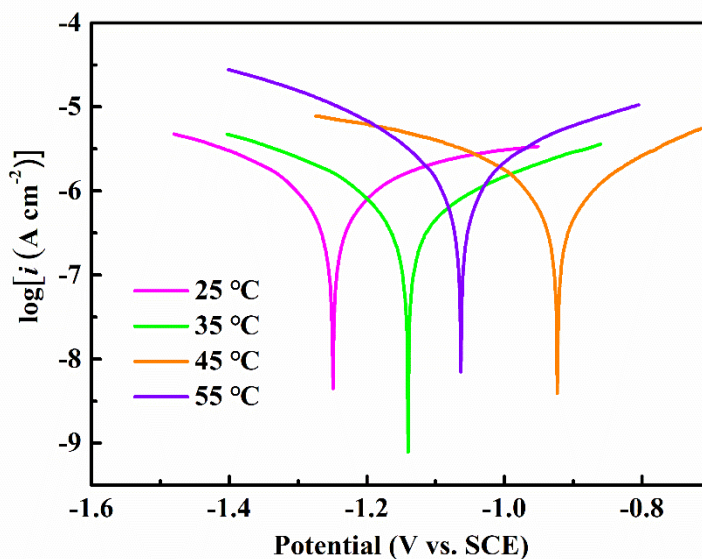


Figure 4. Potentiodynamic curve of aluminum immersed in 0.1 mM acetic acid solution for 5 d

Table 4. polarization curve fitting parameters of aluminum immersed in 0.1 mM acetic acid solution for 5 d

Temperature (°C)	Corrosion potential E_{corr} (V)	Corrosion current density I_{corr} ($\mu\text{A cm}^{-2}$)
25	-1.248	0.337
35	-1.094	0.511
45	-0.921	0.908
55	-1.046	1.651

3.2.2 EIS analysis

The solution temperature had a great influence on the aluminum corrosion in Figure 5. With the increase of solution temperature, the R_s and R_f decreased significantly, while the C_f and C_{dl} increased. From the activation energy of aluminum corrosion reaction, it was found that aluminum corrosion was a process of absorbing energy. On the one hand, the higher solution temperature accelerated the reaction. On the other hand, it shifted the corrosion reaction equilibrium to the right, resulting the corrosion resistance of aluminum became worse. This was consistent with the above conclusion.

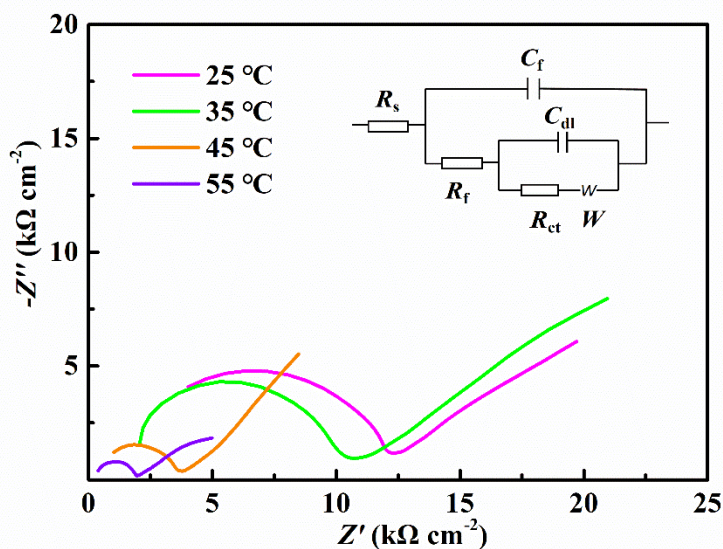


Figure 5. EIS curves of aluminum immersed in 0.1 mM acetic acid solution for 5 d

Table 5. Fitting EIS parameters of aluminum immersed in 0.1 mM acetic acid solution for 5 d

Temperature (°C)	R_s ($\text{k}\Omega \text{ cm}^{-2}$)	C_f (nF cm^{-2})	R_f ($\text{k}\Omega \text{ cm}^{-2}$)	C_{dl} ($\mu\text{F cm}^{-2}$)	R_{ct} ($\text{k}\Omega \text{ cm}^{-2}$)	W ($\mu\Omega \text{ cm}^{-2}$)
25	0.898	12.870	6.565	1.620	9.590	26.970
35	0.657	4.840	0.553	0.270	8.769	23.260
45	0.437	1.217	0.219	0.328	3.082	36.930
55	0.290	1.584	0.354	0.416	1.633	74.330

3.2.3 Physical characterization

To further explore the corrosion law of aluminum surface in acetic acid solution, the SEM images was carried out (Figure 6). The 1 cm² aluminum foils were immersed in 0.1 mM acetic acid solution at various temperatures for 5 d. After that, the aluminum foils were removed, washed with distilled water and anhydrous ethanol for three times, and finally stored in a sealed bag.

The aluminum surface was smooth and almost no corrosion occurs after soaking at 25 °C for 5 d. With the increase of solution temperature, the corrosion of aluminum surface began to appear and the corrosion intensified gradually. With the temperature rising to 55 °C, there was an obvious corrosion pit on the aluminum surface. And the corrosion pits were tapered inward, indicating the corrosion was from the surface to the inside. These results showed that the temperature increase accelerated the aluminum corrosion.

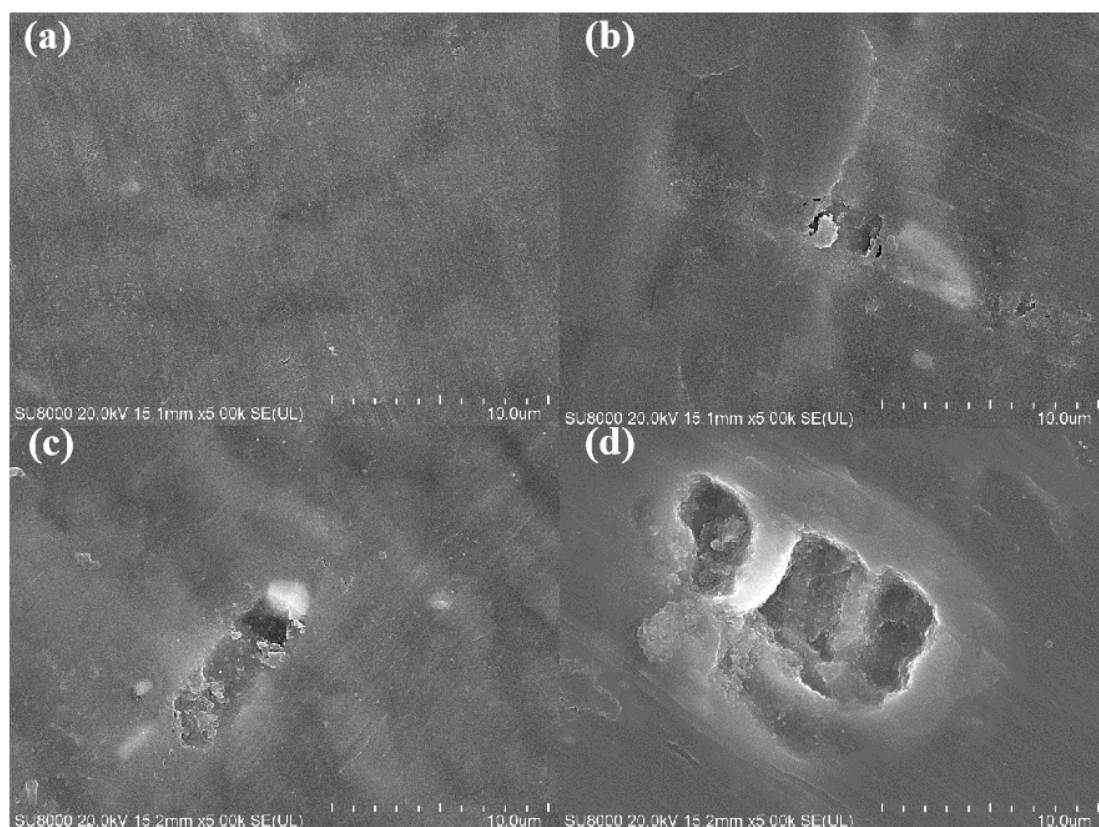


Figure 6. SEM images of aluminum immersed in 0.1 mM acetic acid solution for 5 d at 25 (a), 35 (b), 45 (c), 55 °C (d).

The XRD patterns of aluminum immersed in 0.1 mM acetic acid solution at various temperatures for 5 d were shown in Figure 7. The aluminum peaks of all samples could correspond to the standard card Al (PDF#01-1176). When the temperatures of acetic acid solution were 45 °C and 55 °C, the peaks at 25 °C corresponded well to the peak of the standard card Al(OH)₃ (PDF#37-1377). Therefore, it could be judged that the corrosion product contains Al(OH)₃. This was consistent with the corrosion products of aluminum in the atmosphere and in humid environment [19]. However, the peak of Al(OH)₃ could not be observed at lower temperature, owing to the aluminum had stronger corrosion resistance and

produced less $\text{Al}(\text{OH})_3$ at lower temperature. In addition, the peak of Al_2O_3 could hardly be observed in the XRD patterns, because the Al_2O_3 corrosion product was very little, almost all were in the form of $\text{Al}(\text{OH})_3$.

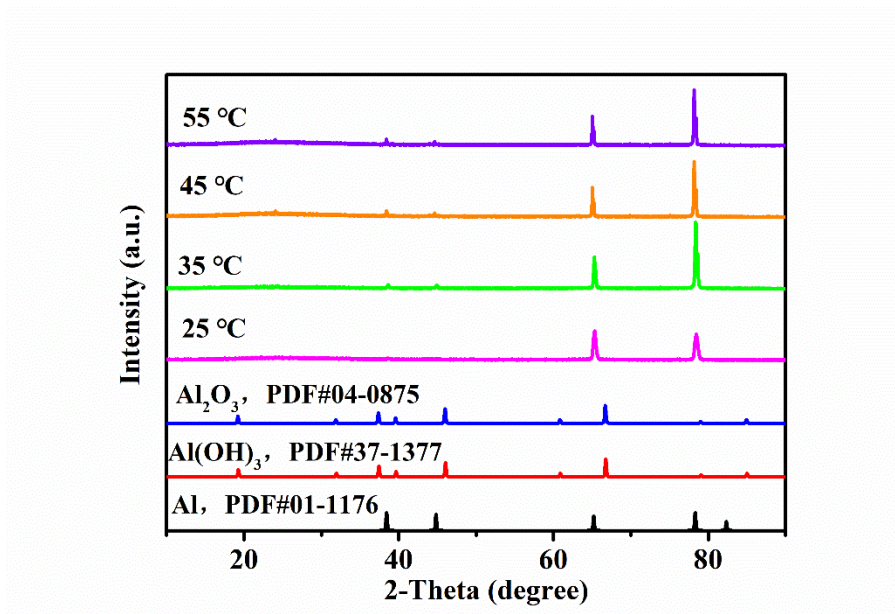


Figure 7. XRD patterns of aluminum immersed in 0.1 mM acetic acid solution with various temperatures for 5 d

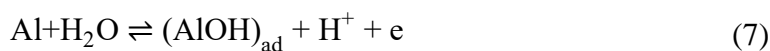
3.3 Corrosion mechanism aluminum in acetic acid solution

A layer of oxide film could be formed on the aluminum surface under natural conditions, and the oxide film had good corrosion resistance and was not easy to corrosion in general. However, in the natural environment, the metal aluminum was easily affected by the ions in the solution, leading to the defects of the oxide film. Additionally, the H^+ in the solution could further corrode the aluminum through the defects, thus forming a corrosion battery with the aluminum as the anode and the oxide film as the cathode [20-22]. The aluminum corrosion in acetic acid solution was a transition chemical reaction process, and its reaction mechanism could be explained by the transition state theory. The aluminum corrosion process was shown in Figure 8.

According to the experimental results, the following reactions existed in the cathode [23-26].



Equation 5 was the control step of the cathodic reaction. The anodic reactions were as follows.



The H^+ in the solution was adsorbed on the active center of aluminum surface, and the adsorbed aluminum atom lost electrons, turning the hydrogen ion into a hydrogen atom. The hydrogen atom formed a composite corrosion product AlH on the aluminum surface and then AlH was desorbed into the solution. According to the transition state theory of chemical reaction, the reactants adsorbed on the active center of the aluminum surface formed an unstable activation complex in the transition state, and then decomposed into corrosion products [27-29].

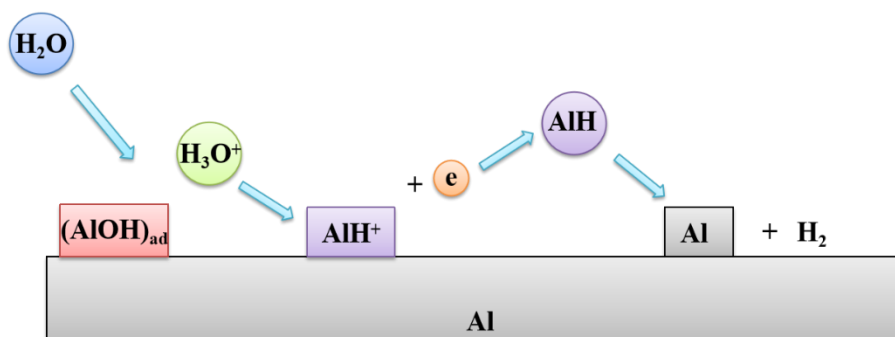


Figure 8. Aluminum corrosion process in acetic acid solution with low concentration

With the increase of acetic acid concentration, the concentration of ionized H^+ in the solution increased. According to the equilibrium theory of reversible reaction, the equilibrium of Equations 4, 5 shifted to the right, resulting in more compound corrosion product AlH. Meanwhile, the increase of AlH concentration also accelerated the aluminum corrosion. Therefore, the higher acetic acid concentration, the worse the corrosion resistance of aluminum.

While, with the increase of solution temperature, the corrosion reaction accelerated. In addition, the aluminum corrosion was a transitional chemical reaction, and the corrosion and dissolution of aluminum were an endothermic process, so the increase of temperature shifted the reaction equilibrium to the direction of forming corrosion products, thus reducing the corrosion resistance of aluminum.

4. CONCLUSION

In this work, the concentration and temperature effect of aluminum corrosion in acetic acid solution with low concentration were studied. With the same solution temperature, the aluminum corrosion resistance decreased with the concentration of acetic acid increased from 0 mM to 1 mM. Meanwhile, aluminum corrosion occurred in acetic acid solution, its activation energy was always negative, indicating the aluminum corrosion was the endothermic reaction. The aluminum corrosion resistance decreased with the increase of solution temperature, leading to the aggravation of aluminum corrosion, and the corrosion pits obviously appeared on the aluminum surface. The aluminum corrosion in low concentration acetic acid solution was a transition chemical reaction process, which consisted of four processes (diffusion \rightarrow surface adsorption \rightarrow surface reaction \rightarrow desorption). The main corrosion product of aluminum in acetic acid solution was $Al(OH)_3$ From the XRD patterns.

References

1. N. Flourentzou, V.G. Agelidis, G.D. Demetriades, *IEEE T. Power Electr.*, 24 (3) (2009) 592. <https://doi.org/10.1109/TPEL.2008.2008441>
2. B.V. Eeckhout, D.V. Hertem, M. Reza, K. Srivastava, R. Belmans, *Euro. Trans. Electr. Power*, 20 (5) (2010) 661. <https://doi.org/10.1002/etep.359>
3. A. Kalair, N. Abas, N. Khan, *Renew. Sust. Energ. Rev.*, 59 (2016) 1653. <https://doi.org/10.1016/j.rser.2015.12.288>
4. Y. Jing, Z. Ren, K. Ou, J. Yu, *Proceedings. International Conference on Power System Technology*, 1 (2002) 538. <https://doi.org/10.1109/ICPST.2002.1053600>
5. J.Y. Jin, S.I. Hong, *Mater. Sci. Eng. A*, 596 (2014) 1. <https://doi.org/10.1016/j.msea.2013.12.019>
6. Y.H. Qian, Y.Y. Zhou, C.W. Xu, *Adv. Mater. Res*, 354-355 (2011) 1157. <https://doi.org/10.4028/www.scientific.net/AMR.354-355.1157>
7. P. Cui, S. Guan, J. Guo, G. Wang, H. Wang, J. Chen, K. Huang, M. Geng, W. Yang, L. Deng, *IOP Conference Series: Materials Science and Engineering*, 768 (6) (2020) 062104. <https://doi.org/10.1088/1757-899X/768/6/062104>
8. I. Weber, B. Mallick, M. Schild, S. Kareth, R. Puchta, R. Eldik, *Chem. Eur. J.*, 20 (38) (2014) 12091. <https://doi.org/10.1002/chem.201400165>
9. J. Li, L. Hao, F. Zheng, X. Chen, S. Wang, Y. Fan, *Int. J. Electrochem. Sci.*, 15 (6) (2020) 5320. <https://doi.org/10.20964/2020.06.04>
10. L. Hao, F. Zheng, X. Chen, J. Li, S. Wang, Y. Fan, *Materials*, 13 (3) (2020) 779. <https://doi.org/10.3390/ma13030779>
11. L. Hao, J. Dai, Z. Huang, C. Lei, F. Zheng, J. Li, Y. Fan, S. Wang, *Int. J. Electrochem. Sci.*, 16 (5) (2021) 210529. <https://doi.org/10.20964/2021.05.20>
12. D. Li, Y. Shi, H. Xu, Y. Chen, P. Zhou, X. Li, W. Feng, S. Wang, *Int. J. Electrochem. Sci.*, 13 (10) (2018) 9346. <https://doi.org/10.20964/2018.10.61>
13. D. Li, Z. Shi, H. Xu, Y. Chen, W. Feng, Z. Qiu, H. Liu, G. Lv, S. Wang, Y. Fan, *Int. J. Electrochem. Sci.*, 14 (4) (2019) 3465. <https://doi.org/10.20964/2019.04.47>
14. F. Zheng, L. Hao, J. Li, H. Zhu, X. Chen, Z. Shi, S. Wang, Y. Fan, *Int. J. Electrochem. Sci.*, 14 (8) (2019) 7303. <https://doi.org/10.20964/2019.08.69>
15. Y. Tian, H. Li, S. Wang, Y. Fan, *Mater. Corros.*, 72 (12) (2021) 1899. <https://doi.org/10.1002/maco.202112453>
16. D. Cicolin, M. Trueba, S.P. Trasatti, *Electrochim. Acta*, 124 (2014) 27. <http://doi.org/10.1016/j.electacta.2013.09.003>
17. H. Li, L. Zhang, S. Wang, J. Yu, *Int. J. Hydrogen Energ.*, 44 (54) (2019) 28556. <https://doi.org/10.1016/j.ijhydene.2019.09.155>
18. T. Zhang, X. Liu, Y. Shao, G. Meng, F. Wang, *Corros. Sci.*, 50 (2008) 3500. <https://doi.org/10.1016/j.corsci.2008.09.033>
19. J. Wysocka, S. Krakowiak, J. Ryl, K. Darowicki, *J. Electroanal. Chem.*, 778 (2016) 126. <https://doi.org/10.1016/j.jelechem.2016.08.028>
20. J. Larminie, J. Lowry, (2003), *Electric Vehicle Technology Explained*, John Wiley & Sons, 2003. <https://doi.org/10.1002/0470090707>
21. D. Moosbauer, S. Zugmann, M. Amereller, H.J. Gores, *J. Chem. Eng. Data*, 55 (5) (2010) 1794. <https://doi.org/10.1021/jc900867m>
22. B.C. Bunker, G.C. Nelson, K.R. Zavadil, J.C. Barbour, F.D. Wall, J.P. Sullivan, C.F. Windisch, M.H. Engelhardt, D.R. Baer, *J. Phys. Chem. B*, 106 (18) (2002) 4705. <https://doi.org/10.1021/jp013246e>
23. M.-D. Chen, K.-L. Han, N.-Q. Lou, *Chem. Phys. Lett.*, 357 (5-6) (2002) 483. [https://doi.org/10.1016/S0009-2614\(02\)00585-7](https://doi.org/10.1016/S0009-2614(02)00585-7)
24. P.B. Mathur, T. Vasudevan, *Corrosion*, 38 (3) (1982) 171. <https://doi.org/10.5006/1.3579270>

25. M. El-Batouti, *Anti-Corros. Method. M.*, 43 (2) (1996) 20. <https://doi.org/10.1108/eb007389>
26. S.A. El-Shazly, A.A. Zaghoul, M.T. Mohamed, R.M. Abdullah, *Anti-Corros. Method. M.*, 42 (4) (1995) 9. <https://doi.org/10.1108/eb007363>
27. Y. Ma, Y. Li, F. Wang, *Corros. Sci.*, 51 (8) (2009) 1725. <https://doi.org/10.1016/j.corsci.2009.04.024>
28. F. Corvo, T. Perez, L.R. Dzib, Y. Martin, A. Castañeda, E. Gonzalez, J. Perez, *Corros. Sci.*, 50 (1) (2008) 220. <https://doi.org/10.1016/j.corsci.2007.06.011>
29. H. Tamura, *Corros. Sci.*, 50 (7) (2008) 1872. <https://doi.org/10.1016/j.corsci.2008.03.008>

© 2022 The Authors. Published by ESG (www.electrochemsci.org). This article is an open access article distributed under the terms and conditions of the Creative Commons Attribution license (<http://creativecommons.org/licenses/by/4.0/>).